



HAL
open science

Properties of the Nili Fossae Olivine-phyllsilicate-carbonate lithology

Adrian J. Brown, R.C. Wiens, P.C. Pinet, Y. Liu, E. Cloutis, J.M. Madariaga,
J.M. Comellas, M. Schmidt, J.I. Simon, G. Poggiali, et al.

► **To cite this version:**

Adrian J. Brown, R.C. Wiens, P.C. Pinet, Y. Liu, E. Cloutis, et al.. Properties of the Nili Fossae Olivine-phyllsilicate-carbonate lithology. 54th Lunar and Planetary Science Conference 2023, Mar 2023, The Woodlands (Texas), United States. hal-04283127

HAL Id: hal-04283127

<https://hal.science/hal-04283127>

Submitted on 13 Nov 2023

HAL is a multi-disciplinary open access archive for the deposit and dissemination of scientific research documents, whether they are published or not. The documents may come from teaching and research institutions in France or abroad, or from public or private research centers.

L'archive ouverte pluridisciplinaire **HAL**, est destinée au dépôt et à la diffusion de documents scientifiques de niveau recherche, publiés ou non, émanant des établissements d'enseignement et de recherche français ou étrangers, des laboratoires publics ou privés.

Properties of the Nili Fossae Olivine-phyllsilicate-carbonate lithology

A.J. Brown¹, R.C. Wiens², P.C. Pinet³, Y. Liu⁴, E. Cloutis⁵, J.M. Madariaga⁶, J.M. Comellas⁷, M. Schmidt⁸, J.I. Simon⁴, G. Poggiali⁷, J.D. Hernandez-Montenegro⁴, ¹Plancius Research, MD (adrian.j.brown@nasa.gov) ²Purdue University, IN. ³IRAP, Toulouse, France. ⁴CalTech-NASA JPL. ⁵Univ. of Winnipeg, Canada. ⁶University of the Basque Country, Leioa, Spain, ⁷Univ. of Hawai'i ⁸Brock Univ, Ontario, ¹⁰INAF, Italy

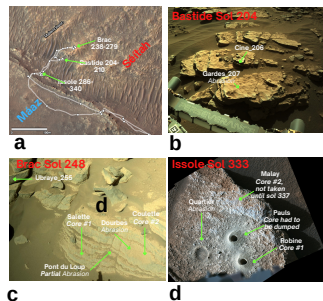


Fig. 1 Visual summary of the traverse through the Séítah formation and the three key workspaces.

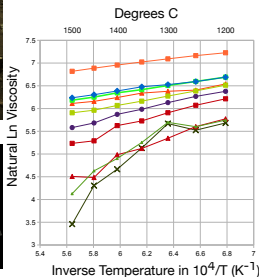


Fig 2. Arrhenius plot of Bottinga-Weill viscosity vs inverse temperature for Maaz (yellow), Séítah (cyan) and Artuby (dark green) compared to terrestrial standards.

Takeaways:

- * We used CRISM and in situ data from the Mars2020 rover to examine the properties and emplacement of the olivine-clay-carbonate lithology.
- * We focus on the viscosity of the unit based on geochemical elemental abundances of the Séítah olivine cumulate rock.
- * We show that clay is also present in the olivine-carbonate lithology. We used VISIR instrument to observe the 2-2.5 micron region of the spectrum to look for bands indicative of clays in the olivine cumulate rocks of Séítah.
- * We have used the SuperCam LIBS instrument to determine Séítah's low (<4wt %) Al₂O₃ - allowing us to eliminate clays with aluminum in their structure.
- * Using elemental abundances from the SuperCam LIBS, we derive the viscosity of the lava flow that replaced the Séítah cumulate, and find it to be exceedingly low.
- * Based on this observation, we hypothesize that the Séítah unit was formed by a flood lava similar to the Columbia Ridge basalt. We hypothesize that the olivine cumulate was formed at the base of a lava lake within Jezero crater that was part of a region-wide unit.

The Mars 2020 rover landed at Jezero crater on February 18, 2021 [1]. Since then, the rover has traveled around the “Séítah” region [2] and has collected data from the Mastcam-Z, Supercam, PIXL and SHERLOC instruments that has led to insights into the formation of the olivine-clay-carbonate bearing rocks that were identified from orbit [3,4]. Here we discuss three questions: 1) What have we learned about the olivine-clay-carbonate unit? 2) What terrestrial analogs exist for the unit? 3) Why do the rocks have a thinly layered morphology? We shall briefly mention instrumental measurements which provide important information regarding the olivine bearing rock at Séítah. The findings of this abstract are the subject of a paper submitted to the Mars2020 JGR Special section. We have examined orbital (CRISM) and in situ data from the Mars2020 rover focused on deepening our understanding of the properties and emplacement of the olivine-clay-carbonate lithology. We particularly focus on the estimated viscosity of the unit based on geochemical elemental abundances of the Séítah olivine cumulate rock.

We used a Venn-diagrammatic approach to determine the relationships between the olivine, clay and carbonate in the olivine clay-carbonate in the CRISM 40FF image (which covers the west side of the crater, see Figure 6). We were able to show that clay is also present in the olivine-carbonate lithology. We have now used in situ observations to help identify the clay. We have used the SuperCam VISIR instrument onboard the M2020 rover to observe the 2-2.5 micron region of the spectrum to look for bands indicative of clays in the olivine cumulate rocks of Séítah. Using the appearance of the 2.38 and 2.46 micron bands we have been able to narrow the search to clays with metal-OH features. Finally, we have used the SuperCam LIBS instrument to determine the low (<4wt %) Al₂O₃ thereby allowing us to eliminate clays with aluminum in their structure. The only remaining candidates are talc and Mg-rich serpentine, and we will further discuss ideas for telling these two minerals apart. Using elemental abundances derived by the LIBS instrument on

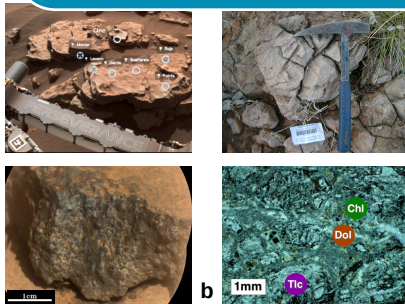


Fig. 4 - SuperCam RMI of target Cine showing olivine cumulate texture at mm scale. (top) Bastide workspace, location of Cine relative to Garde, rover arm for scale. b.) (bottom) Thin section of talc-carbonate sample AJB0503100 from Brown [8] with mm size talc (Tlc) replacing olivine, dolomite (Dol) and chlorite (Chl) identified using electron microprobe. (top) Context image for target AJB0503100 with hammer for scale.

SuperCam, we have used the heuristic Bottinga-Weill approach [5] to derive the viscosity of the lava flow that replaced the Séítah cumulate [6], and find it to be exceedingly low. Based on this observation, we hypothesize that the Séítah unit was formed by a flood lava similar to the Columbia Ridge basalt [7]. We hypothesize that the olivine cumulate was formed at the base of a lava lake within Jezero crater that was part of a Nili Fossae region-wide unit.

What have we learned about the Olivine-clay- carbonate lithology? The olivine-clay-carbonate lithology is among the best-documented rock types in Jezero crater and the surrounding watershed [3] and is potentially among the most astrobiologically compelling units in the region [9,10]. From orbital VNIR reflectance spectra, the unit contains abundant olivine (Fo#45-66) in large grains (>500 μm, based on band saturation) accompanied by clay and carbonate minerals [3], and its crater retention age is ~3.82 Ga [11]. Several potential origins of the olivine-rich unit are possible: 1) a density segregated melt associated with a lava flow or lake; 2) a pyroclastic density current (PDC) at low temperature [11]; 3) tephra fall [12]; or 4) some combination of all of the above, see also [13]. The transition from primary volcanic deposit to the olivine-carbonate-clay could have been from deuteric serpentinization and talc-carbonation [8] perhaps caused by late Noachian CO₂ outgassing [14]. It is also possible that the olivine was altered to carbonate when it was exposed to a thick CO₂-rich Noachian atmosphere [15]. Discrimination between these formation and alteration histories is critical to advancing our understanding of Noachian mantle circulation [16].

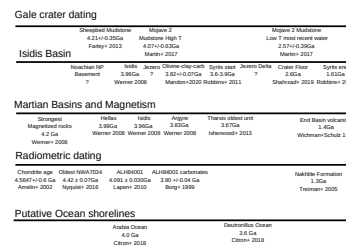


Fig. 7 Timeline of events relevant to the emplacement and retention of the olivine-clay-carbonate lithology.

Terrestrial analog of komatiite sequence: Here we consider a low viscosity lava flow or lake which density-segregated into a layered cumulate. Figure 4 shows two examples from the ultramafic Archean stromatolite-bearing Dresser Formation in Western Australia. Olivine replaced by serpentine and talc-carbonate are seen in a petrographic thin section in the image. Similarities with the olivine-clay-carbonate include the mm size cumulate textures and mineralogy, in this case the olivine is replaced by talc or serpentine. We are using the elemental abundances of the Supercam LIBS instrument to calculate the viscosity of the olivine-clay-carbonate unit at Séítah and Figure 2 compares Séítah with a terrestrial dunite, the CF-FR and Artuby rocks from [6]. For reference, terrestrial granite and diorite are given. The calculated viscosity of the Séítah rocks is lowest among all these examples, and we suggest this might explain some of the characteristics of this rock, including thin layering seen in Figure 1.

Take away messages: 1) We have outlined how the SuperCam LIBS and VISIR instruments of the Perseverance rover are being used to increase our understanding of this unit and determine their variations around Jezero. 2) We have outlined the case for a komatiitic succession of rocks as an information-rich analog for the olivine-bearing rocks at Séítah. 3) We have calculated viscosities for the olivine-bearing rocks and these indicate a low viscosity that may help explain the thin layering and morphological characteristics of these rocks.

References: [1] Farley, K.A.+ (2020) SSR 216 142 [2] Stack, K.M.+ (2020) SSR 216 127 Sun, V. and Stack, K.M. USGS SIMap #3464 [3] Ehlmann B.+ (2008) *Science* 322 1828 Goudge, T.+ (2015) *JGR* 120 775-808 [4] Brown, A.J.+ (2020) *JGR* 125 2019JE006011; Brown, A.J.+ (2010) *EPSL* 297 174-182 [5] Bottinga and Weill, 1972 *American J. of Science* 272 438-475; McGetchin and Smythe J.R. (1978) *Icarus* 34 512-536 [6] Wiens, R.+ (2022) *Science Advances*, 3399; Udry, A.+ (2022) *JGR* special section; Mandon, L.+ (2022) *JGR* special section; [7] Plescia, J. (1990) *Icarus* 88 465-490 [8] Brown, A.J. (2006) *PhD thesis*, Macquarie Univ. [9] Worster+ (1993) *JGR* 98. [10] Horgan, B.+ (2020) *Icarus* 339 113526 [11] Mandon+ (2020) *Icarus* 336 113436 [12] Kremer, C.+ (2019) *Geology* 111 E02S10 [13] Ravanis, E.+ (2022) this meeting [14] Grott, M.+ *EPSL* 308 391-400 [15] Pollack, J.B.+ (1987) *Icarus* 71 203-224 [16] Hirschmann, M.M.+Withers, A.C. *EPSL* 270 147-155 Kiefer, W.S. (2003) *MAPS* 38 1815-1832

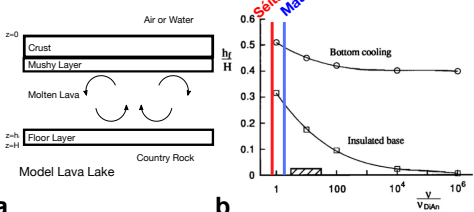


Figure 3 - 1) nermal model of a lava flow and lava lake. a.) 1-mat tractional height of floor layer, h_f , where crystals accumulate (relative to the height of the chamber height, H) plotted against the lava viscosity (normalized relative to liquid diopside). Two cases are shown, one in which bottom cooling occurs, and one in which it does not (insulated base). The dashed box indicates the viscosity of typical terrestrial basalt relative to a pure diopside melt, after [9]. The Séítah and Maaz viscosities calculated in this paper are schematically shown on the plot.

Fig 5 - Dourbes with tailings on Sol 255 after abrasion in the Brac workspace. Note brightness of tailings relative to original rock surface. b.) Spectra of tailings compared to the original rock surface. Note the presence of the 2.46 μm band in the tailings spectra c.) SuperCam RMI image of Dourbes tailings after abrasion.

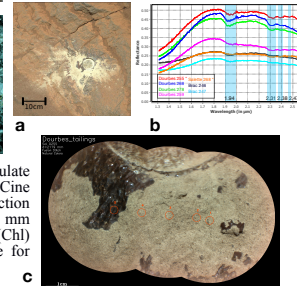


Fig 6 - HRL40FF 0.905 μm, 2.31 μm, 2.5 μm, 2.38 μm band maps. “MC” is location of marginal carbonates. (below) Venn diagram of olivine-clay-carbonate detections for HRL40FF showing pixels containing olivine, clay and carbonate.

